

Failure Probability and Reliability of Hatch Cover of Bulk Carrier Subjected To Lateral Pressure Load



Abdolhossein Mohammadrahimi, Mesbah Sayebani

One of the situations that may cause severe damage and even sinking of bulk bulkheads is the destruction of the hatch cover and as a consequence of the ship's waterlogging. This destruction may be due to heavy loads on the page, such as shock wave loads. Considering this, it is very important to investigate the possibility of structural failure in this situation. In this paper, using a MATLAB programming language developed for the FORM method, we have tried to summarize the reliability analysis on two models of bulk carrier storage models. To achieve this, first, the algorithm of the method of expression, and then the limit state function of this failure state and its components are described, then the probability of failure of these two models of the storage compartment is calculated.

Keywords: FORM method; reliability; Health index; Limit state function.

I. INTRODUCTION

In the 1980s, the MV Derbyshire, a bulk carrier, drowned near Lake Okinawa, Japan, due to the destruction of the hatch cover and flooded cargo holds. Afterwards, in order to prevent similar occurrences, different marine organizations decided to increase the strength of the hatch covers in bulk carriers, so that the decision was made and approved by the International Maritime Organization (IMO). Subsequently, this issue was raised at the International Association of Classification Societies (IACS), and the UR, S21 was required to increase the strength of the hatch cover and was required since 1997. Different types of ships have occurred in different parts of the ship, and each of these phenomena can cause a particular damage to the ship's components. One of these destructive phenomena is the impact on the deck in the ship's chest, also known as the Green Sea. This phenomenon occurs when the height of the wave in the ship's chest is higher than the height of the structure (with respect to the structure of the structure in the chest) and causes the wave to fall in the chest of the ship (Fig. 1).

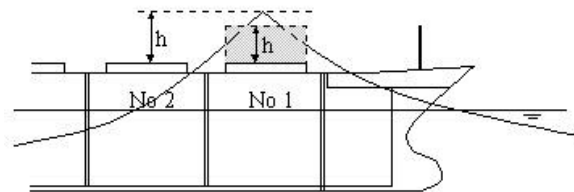


Fig. 1. Schematic diagram of the phenomenon of wave loss in the ship's chest

In this paper, the limit state function is described first in relation to the failure of the hatch cover. Then, a series of large-scale elastoplastic analyzes on the hatch cover of bulk carrier was carried out using the finite element method using the ANSYS software to calculate the loading capacity of the ship's hold door for a few specific models. Finally, the probability of annual damage to the hatch cover is calculated using reliability methods.

II. CALCULATION OF SUSTAINABLE PRESSURE BY HATCH COVER

In this paper, a hatch cover model for a Handy size ship and another hatch cover model for a Panamax ship has been modeled and analyzed. Handy size and Panamax ships are two types of bulk carriers. The folding type is used for the hatch cover of the Handy size. And as shown in Fig. 2, for each hatch cover of this bulk carrier, 4 folding doors are considered. The sliding type is used for the hatch cover of the Panamax.

According to Fig. 3, each hatch cover of this bulk carrier contains two sliding type doors, each of which has a simple support on the three edges, and the fourth edge is free.

Generally, each hatch cover is designed in accordance with ICLL 1966 [3] or IACS 1997 [4]. Dimensions and sizes of the two models of the considered hatch covers are shown in Fig.4. In this figure, the symbol "H" means high strength steel with a yield stress of 313.6 MPa. Each material of panels without the symbol "H" also means the soft steel with a yield stress of 235.2 MPa. In these analyzes, the stress-strain curve of the used materials is considered as elastic-perfectly plastic, and the margin of corrosion thickness is also specified for all parts in this design and its value is defined as following.

hatch cover folding door: 2mm for top and bottom sheets and 1.5mm for other structural components.

Revised Manuscript Received on June 30, 2020.

* Correspondence Author

Abdolhossein Mohammadrahimi*, Department of Maritime Engineering, Amirkabir University of Technology, Hafez Ave, Tehran, Iran. Email: a.mohammadrahimi@aut.ac.ir, Mobile No: +989133435193

Mesbah Sayebani, Department of Maritime Engineering, Amirkabir University of Technology, Hafez Ave, Tehran, Iran. Email: msaybani@aut.ac.ir

© The Authors. Published by Blue Eyes Intelligence Engineering and Sciences Publication (BEIESP). This is an open access article under the CC BY-NC-ND license (<http://creativecommons.org/licenses/by-nc-nd/4.0/>)

Failure Probability and Reliability of Hatch Cover of Bulk Carrier Subjected To Lateral Pressure Load

hatch cover sliding door: 2mm for all structural components.

The thicknesses shown in Fig.4 are specified with regard to the margin effect of the corrosion thickness.

In order to model the hatch cover, 4-node Shell143 element is used in the Ansys software, which allows the analysis of large shape changes and non-linear materials.

Various shock loads, such as the shock of a wave, may be applied to a hatch cover. These loads are mostly dynamic in their nature. In semi-static analyzes, such as different standards, dynamic loads on structures are considered statics. Here, the shock loads of the wave are assumed as uniformly static pressure on the hatch cover.

In the elastoplastic analysis, this static pressure is introduced gradually, vertically to the upper plate of the hatch cover. In the current analysis, the secondary boosters around the hatch cover have not been modeled, but the effect of these boosters has been modeled on the support of the hatch cover as a simple support. The edges of the hatch cover that are not on these secondary boosters are modeled freely.

After performing various analyzes on the hatch cover of various bulk carriers, the lateral pressure diagram based on the displacement of the middle node of the upper plate of the hatch cover is presented for two different doors. The pressure-displacement curve is linear in lower pressures, but with increasing lateral pressure, it will gradually become nonlinear, so that the lateral pressure variation will be more significant and these conditions are considered as the sheet destruction conditions.

In fact, it is difficult to determine the sheet destruction load in these conditions. In order to obtain the destruction load of the hatch cover 2, tangent lines are plotted on the pressure-displacement curve in accordance with Fig. 5, which will be indicative of the elastic and plastic behavior of the reinforced sheets of the hatch cover.

And the critical destruction load of the hatch cover is considered to be equal to the pressure of collision of the two lines above [5].

By applying and increasing the lateral pressure on the folding type hatch cover, firstly its upper reinforced plate gets into localized buckling. With increasing lateral pressure, this localized buckling increases and also extends to longitudinal boosters such as the surrounding walls.

At the same time as the lateral pressure is applied, the tensions of the bottom plate of the hatch cover are increased and the materials enter the plastic zone in this area. The tension development in the hatch cover is shown in Fig. 6, with a above view.

In this type of hatch cover, the buckling of the upper plates and longitudinal boosters and the creation of a plastic area on the bottom plate and the boosters connected to it, respectively, create a plastic node in the middle of the hatch cover and, according to the definition, displacement changes to pressure changes in the hatch cover increases. The slip type of the hatch cover is similar to the previous one. The development of stress and deformation for an example of this model is shown in Fig. 7.

Finally, after performing the necessary analyzes, the results of the sustainable pressure of the hatch covers are shown in Table (1).

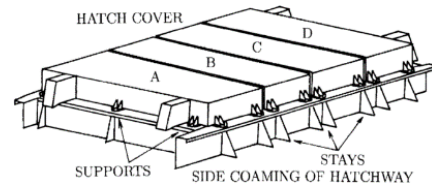


Fig. 2. Slip type of hatch cover [2]

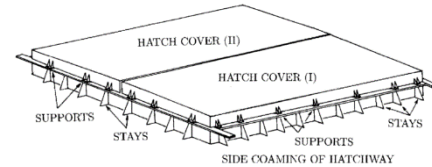
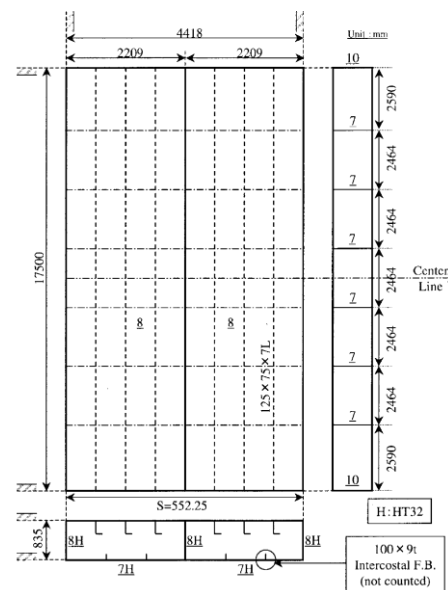
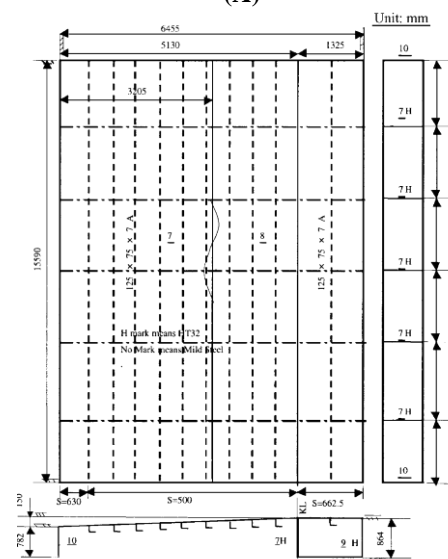


Fig. 3. Sliding type of hatch cover [2]

Fig. 4.



(A)



(B)

Fig. 5. A-Handy size (ICLL), B-Panamax size (ICLL) [2]

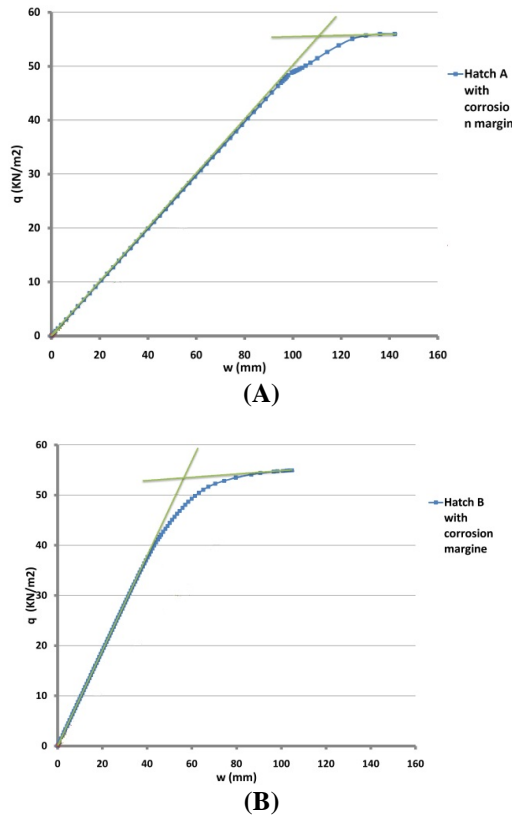


Fig. 5. Lateral pressure diagram based on the displacement of the middle node of the upper plate of the hatch cover A and B [2]

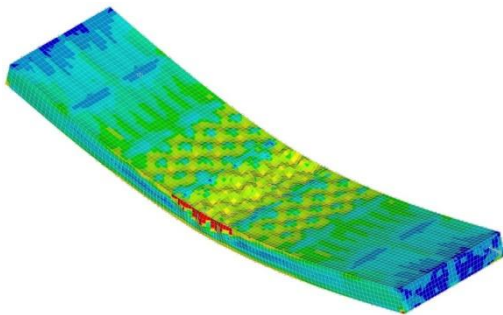


Fig. 6. Deformation and tension development of the hatch cover after the critical load for the hatch cover (A) [2]

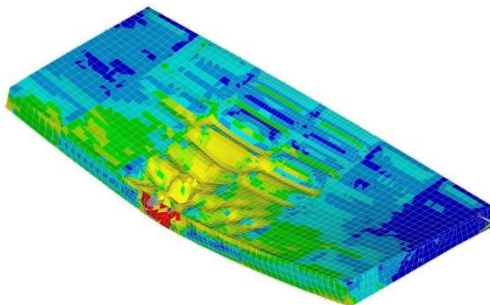


Fig. 7. Deformation and tension development of the hatch cover after the critical load for the hatch cover (B) [2]

Table- I: Name of the Table that justify the values

sustainable load p^c (kN/m^2)	Hatch cover No.
55.90	Hatch cover (A) with margin effect of corrosion thickness
53.50	Hatch cover (B) with margin effect of corrosion thickness

III. RELIABILITY ANALYSIS [6]

The purpose of analyzing the reliability of a structure is to find the probability of its failure. In order to achieve this, firstly, Limit State Function of the structure must be determined in each failure mode. The limit state function of the structure in general conditions can be written as equation (1).

$$G = R - S \tag{1}$$

In this equation, the parameters G, R and S, are respectively, the limiting function, the resistance or the bearing capacity of the structure and the load on the structure. In this situation, if $G < 0$ it indicates the failure of the structure condition. The probability of structure failure is also obtained from equation (2). In this equation, $f_{RS}(r, s)$ indicates Joint Probability Density Function. For a state of resistance loading with a normal and non-dependent distribution, the limit state function is expressed as follows:

$$f_G(g) = \frac{1}{\sigma_g \sqrt{2\pi}} \exp\left[-\frac{1}{2} \left(\frac{g - \mu_g}{\sigma_g}\right)^2\right] \tag{2}$$

And the probability of failure for random variables with normal distribution, is obtained by equation (3)

$$P_f = P(R - S \leq 0) = \tag{3}$$

$$\int_{-\infty}^0 \frac{1}{\sigma_g \sqrt{2\pi}} \exp\left[-\frac{1}{2} \left(\frac{g - \mu_g}{\sigma_g}\right)^2\right] d_G = 1 - \Phi(\beta) = \Phi(-\beta)$$

$$\beta = \frac{\mu_G}{\sigma_G} = \frac{\mu_R - \mu_S}{\sqrt{\sigma_R^2 + \sigma_S^2}} \tag{4}$$

In equation 3, $\Phi(-\beta)$ is the standard normal cumulative function.

In order to solve the probability integral of equation 3, the first order FORM method is used. In 1975, an effective method for determining the reliability index (β) was proposed by Hoesfer-Lind (HL) to search for a design point, that is, the least distance of the limit state function to the center of the normal coordinates system. Accordingly, the failure distance to the center is called as reliability index function, which is defined as follows:

$$\beta = (U^T U)^{\frac{1}{2}}, \quad U \in g(U) = 0 \tag{5}$$

In which the $G(U)$ is the limit state function in the standard normal space of base random variables (U). With regard to the above equation and HL definition, the reliability index on the failure level $G(U) = 0$ is defined as:

$$\beta = \min_{U \in g(U)=0} (U^T U)^{\frac{1}{2}} \quad (6)$$

The above equation is known as the first-order reliability equation, which the point $U^*(u_1^*, u_2^*, \dots, u_n^*)$ on the surface $G(U) = 0$ is called as the design point. According to equation 6, we are facing with an optimization problem with equality constraint which the main goal of optimization problem is to determine the health index. There are different methods and algorithms for solving the problem [7]. The method used in this research is HL method which is developed by Rackwitz and Fiessler, and hence the method is also called HL-RF. Consider the n-dimensional limit state function with random variables with normal and non-dependent distribution X .

$$g(X) = g(\{x_1, x_2, \dots, x_n\}^T) \quad (7)$$

The limit state function can be linear or nonlinear. Using following conversion, the variables are converted into standard form.

$$u_i = \frac{x_i - \mu_{x_i}}{\sigma_{x_i}} \quad (8)$$

With this conversion, the limit state function is converted to the following form:

$$g(X) = g(\{\sigma_{x_1} u_1 + \sigma_{x_2} u_2 + \dots + \sigma_{x_n} u_n + \mu_{x_n}\}^T) = 0 \quad (9)$$

Figure 8 shows the transformation of the fracture surface from space X to the standard space U . the normal vector of a line from the center of the coordinates to the failure point of the point P^* at the point of intersection with this surface, creates the point MPP (Most Probable Failure Point). The distance from the mentioned point to the center of coordinates (shortest distance) represents the health index (β). The first order Taylor series of function $g(U)$ in $MPP U^*$ is as follows:

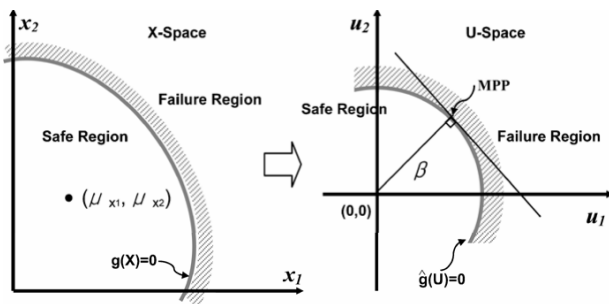


Fig. 8. transformation of the fracture surface from space X to the standard space U

$$g(U) \approx g(U^*) + \sum_{i=1}^n \frac{\partial g(U^*)}{\partial u_i} (u_i - u_i^*) \quad (10)$$

Using the conversion equation 8, it can be written:

$$\frac{\partial \hat{g}(U)}{\partial u_i} = \frac{\partial g(X)}{\partial x_i} \sigma_{x_i} \quad (11)$$

The shortest distance from the coordinates' center to the approximate failure surface in equation 9 is equal to:

$$\cos \theta_{P^*} = \beta = \frac{g(U^*) - \sum_{i=1}^n \frac{\partial g(U^*)}{\partial x_i} \sigma_{x_i} u_i^*}{\sqrt{\sum_{i=1}^n \left(\frac{\partial g(U^*)}{\partial x_i} \sigma_{x_i}\right)^2}} \quad (12)$$

The cosine of the above vector angle is calculated by the following equation:

$$\cos \theta_{x_i} = \cos \theta_{u_i} = -\frac{\frac{\partial g(U^*)}{\partial u_i}}{|\nabla g(U^*)|} = -\frac{\frac{\partial g(X^*)}{\partial x_i} \sigma_{x_i}}{\left[\sum_{i=1}^n \left(\frac{\partial g(X^*)}{\partial x_i} \sigma_{x_i}\right)^2 \right]^{\frac{1}{2}}} \quad (13)$$

α_i is called sensitivity coefficient.

The coordinates of point P^* in the standard coordinates system are calculated as follows:

$$u_i^* = \frac{x_i^* - \mu_{x_i}}{\sigma_{x_i}} = \cos \theta_{x_i} \beta = \beta \cos \theta_{x_i} \quad (14)$$

And the coordinates of point A in the main coordinates system are calculated as follows:

$$x_i^* = \mu_{x_i} + \beta \sigma_{x_i} \cos \theta_{x_i}, (i = 1, 2, \dots, n) \quad (15)$$

By defining the appropriate limit function and performing this repeat algorithm, the health index and the reliability values are calculated. In the first step of the algorithm ($k = 1$), the mean values of the random variables are considered for x_i 's of point $P^* (x_{i,k=1} = \mu_{x_i})$, and then values of β , X_k and U_k are calculated. By proceeding the algorithm, the values obtained for β are convergent and the final value with the desired accuracy is the desired value of β , or the health index.

IV. RELIABILITY OF THE FAILURE STATE OF THE HATCH COVER

In order to investigate the failure probability by the reliability method, firstly, a limit state function must be defined for that failure. For the hypothesized conditions in this paper, we can define the limit function as equation (5).

$$G = p^c - p^d \quad (16)$$

In this equation, p^c is the sustainable pressure by the structure of the hatch cover and p^d is the dynamic pressure applied to the structure of the hatch cover. As mentioned earlier, for calculating P^c , a number of finite element analyzes must be performed on the specified and assumed models of the hatch cover in order to obtain the sustainable pressure of the structure.

The overall calculation procedure of P^c and its conditions will be described in the next section.

In the present analysis, the value of p^c is considered statistically with an average of p^c and the different variation coefficient with normal statistical distribution is considered. The variation coefficient changes based on the change in the properties of the raw materials used in the production of the hatch cover and the change in the manufacturing accuracy and the value of the reliability is calculated based on the variation coefficient. To calculate the reliability using FORM method, the analyzes were carried out by a program in Matlab programming language based on the theory stated in [6].

Different relations for calculating the p^d , are proposed in various maritime codes. Here, the equation provided by the IACS institute (Equation 6) is used [8].

$$p^d = k^{dyn} \cdot \rho \cdot g \cdot (k^{nl} \cdot relu6 - (h - T)) \quad [kN/m^2] \quad (17)$$

In this equation:

k^{dyn} : is the dynamic factor which represents the dynamic to static pressure ratio. Here this factor is considered equal to 1.4.

ρ : Sea water density equal to 1.025 N/m^3

g : Gravity acceleration equal to 9.81 m/s^2

k^{nl} : is the nonlinear factor of vertical motion of the ship's bow, which is considered equal to 0.91

$relu6$: Linear motion at the hatch cover number 1 in the ship's bow and on its central line which is considered 15/15 according to the IACS Regulation [8].

h : Height from reference line to hatch cover (m)

T : Waterline at the hatch cover (m)

V. RELIABILITY ANALYSIS FOR HATCH COVER OF PANAMAX AND HANDY SIZE SHIPS

The limit function G defined by relation (5), is written based on the description P^c and P^d as:

$$G = p^c - k^{dyn} \cdot \rho \cdot g \cdot (k^{nl} \cdot relu6 - (h - T)) \quad (18)$$

In this function, two important statistical variables of ultimate strength and waterline are considered respectively with symbols P^c and T with normal distributions. Under different conditions of construction and design, as well as in different shipping conditions, these normal distributions will change, too. The values of the failure probability and reliability of the two hatch covers of A and B, which are functions of P^c and T , are calculated by changing of standard deviation of these two variables, and the results will be shown in the tables and diagrams below. The mean values of the normal distribution of P^c and T , for the hatch cover A are $55.9 \text{ (kN/m}^2\text{)}$ and 5.5 (m) respectively, and for the hatch cover B are $53.5 \text{ (kN/m}^2\text{)}$ and 10 (m) respectively [2]. The values shown in tables 2 and 3 are calculated based on different values, and the corresponding charts are plotted based on these data. The value of " h " for Handy size is 15.6 (m) and for Panamax is 20.6 (m) .

Table- II: values of the reliability index, reliability, and failure probability for different σ_T 's and σ_{p^c} 's for hatch cover

number (A)										
$\sigma_{p^c} = 0.25$										
σ_T	0.1	0.15	0.2	0.25	0.3	0.35	0.4	0.45	0.5	0.55
β	2.826	1.9	1.429	1.145	0.955	0.819	0.717	0.637	0.574	0.522
P_f	0.0024	0.029	0.076	0.126	0.17	0.206	0.237	0.262	0.283	0.301
$R = 1 - P_f$	0.9976	0.971	0.924	0.874	0.83	0.794	0.763	0.738	0.717	0.699
$\sigma_{p^c} = 2.5$										
σ_T	0.1	0.15	0.2	0.25	0.3	0.35	0.4	0.45	0.5	0.55
β	1.408	1.234	1.073	0.936	0.823	0.731	0.656	0.593	0.541	0.496
P_f	0.08	0.109	0.142	0.175	0.205	0.232	0.256	0.276	0.294	0.31
$R = 1 - P_f$	0.92	0.891	0.858	0.825	0.795	0.768	0.744	0.724	0.706	0.69
$\sigma_{ST} = 1.4$										
σ_{p^c}	0.25	0.5	0.75	1	1.25	1.5	1.75	2	2.25	2.5
β	2.826	2.704	2.533	2.339	2.146	1.963	1.798	1.651	1.522	1.408

Failure Probability and Reliability of Hatch Cover of Bulk Carrier Subjected To Lateral Pressure Load

P_f	0.0024	0.0034	0.0057	0.0097	0.016	0.0248	0.0361	0.0493	0.064	0.08
$R = 1 - P_f$	0.9976	0.9966	0.9943	0.9903	0.984	0.9752	0.9639	0.9507	0.936	0.92
$\sigma_T = 0.55$										
σ_{p^c}	0.25	0.5	0.75	1	1.25	1.5	1.75	2	2.25	2.5
β	0.522	0.521	0.519	0.518	0.515	0.512	0.509	0.505	0.501	0.496
P_f	0.301	0.301	0.302	0.3024	0.303	0.304	0.305	0.3067	0.308	0.31
$R = 1 - P_f$	0.699	0.699	0.698	0.6976	0.697	0.696	0.695	0.6933	0.692	0.69

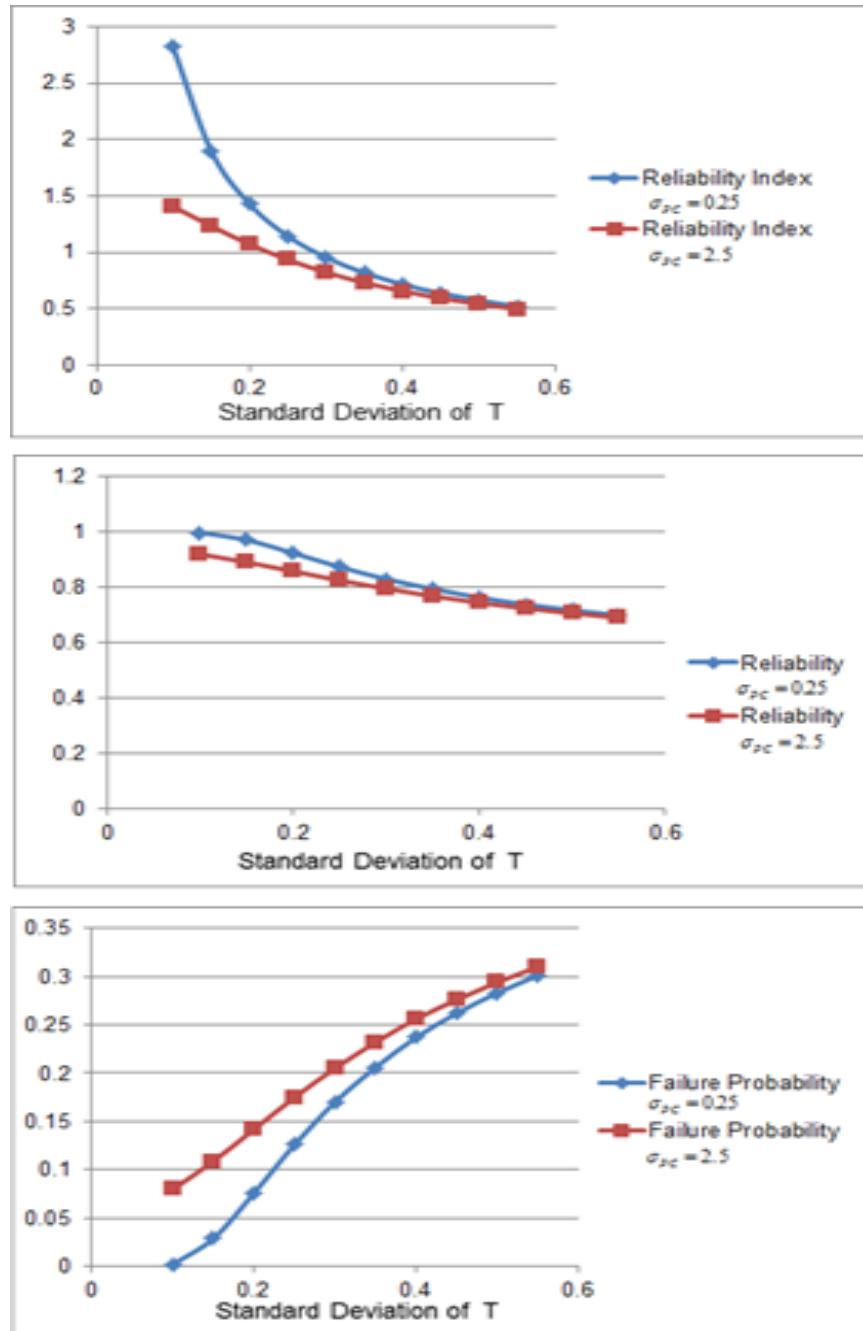


Fig. 9. curves of the reliability index, reliability, and failure probability for $\sigma_{p^c} = 0.25, 2.5$ and different σ_T for hatch cover number (A)

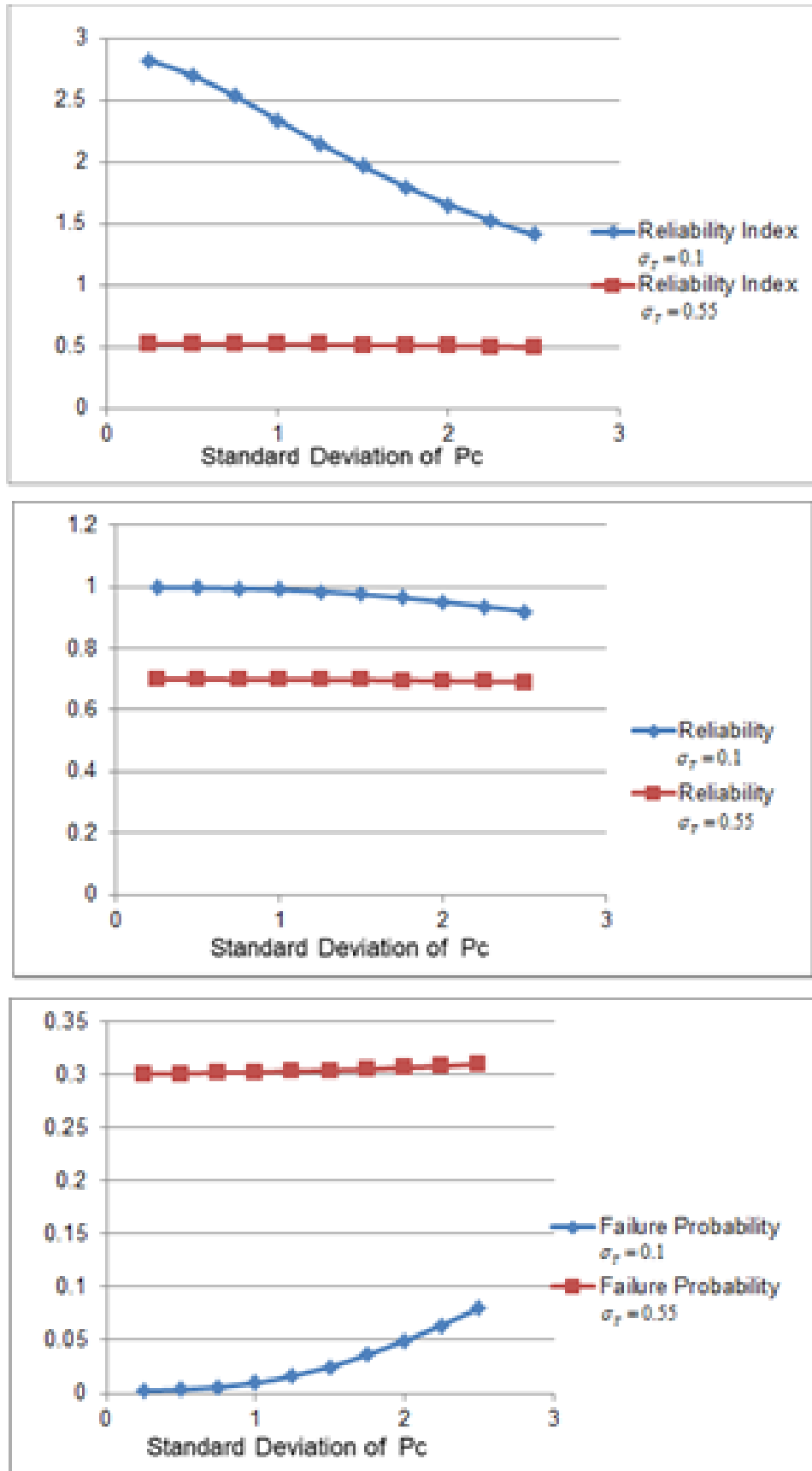


Fig. 10. curves of the reliability index, reliability, and failure probability for $\sigma_T = 0.1, 0.55$ and different σ_{p^c} 's for hatch cover number (A)

Failure Probability and Reliability of Hatch Cover of Bulk Carrier Subjected To Lateral Pressure Load

Table- III: values of the reliability index, reliability, and failure probability for different σ_T 's and σ_{p^c} 's for hatch cover number (B)

$\sigma_{p^c} = 0.25$										
σ_T	0.1	0.2	0.3	0.4	0.5	0.6	0.7	0.8	0.9	1
β	6.07	3.07	2.05	1.54	1.23	1.027	0.88	0.77	0.685	0.616
P_f	0	0.001 1	0.020 1	0.061 8	0.109	0.152	0.189	0.22	0.247	0.269
$R = 1 - P_f$	1	0.998 9	0.979 9	0.938 2	0.891	0.848	0.811	0.78	0.753	0.731
$\sigma_{p^c} = 2.5$										
σ_T	0.1	0.2	0.3	0.4	0.5	0.6	0.7	0.8	0.9	1
β	3.023	2.3	1.77	1.41	1.162	0.985	0.854	0.752	0.672	0.607
P_f	0.001 3	0.010 6	0.038 5	0.079 5	0.123	0.162	0.197	0.226	0.251	0.272
$R = 1 - P_f$	0.998 7	0.989 4	0.961 5	0.920 5	0.877	0.838	0.803	0.774	0.749	0.728
$\sigma_T = 0.2$										
σ_{p^c}	0.25	0.5	0.75	1	1.25	1.5	1.75	2	2.25	2.5
β	3.07	3.035	2.98	2.9	2.82	2.72	2.62	2.5	2.41	2.3
P_f	0.001 1	0.001 2	0.001 5	0.001 8	0.002 4	0.003 3	0.004 4	0.006	0.008	0.010 6
$R = 1 - P_f$	0.998 9	0.998 8	0.998 5	0.998 2	0.997 6	0.996 7	0.995 6	0.994	0.992	0.989 4
$\sigma_T = 0.5$										
σ_{p^c}	0.25	0.5	0.75	1	1.25	1.5	1.75	2	2.25	2.5
β	1.232	1.23	1.225	1.221	1.214	1.21	1.196	1.186	1.174	1.162
P_f	0.109	0.109 4	0.11	0.111	0.112	0.114	0.116	0.118	0.12	0.123
$R = 1 - P_f$	0.891	0.890 6	0.89	0.889	0.888	0.886	0.884	0.882	0.88	0.877

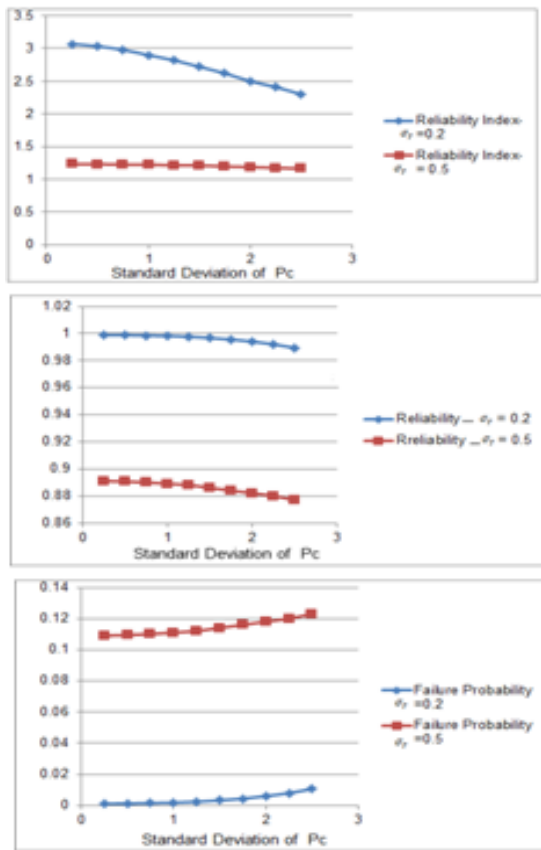


Fig. 11. curves of the reliability index, reliability, and failure probability for $\sigma_{p^c} = 0.25, 2.5$ and different σ_T for hatch cover number (B)

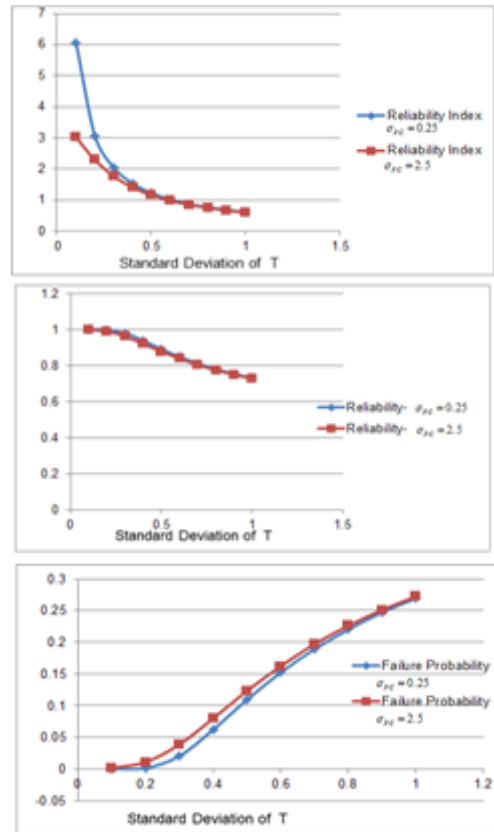


Fig. 12. curves of the reliability index, reliability, and failure probability for $\sigma_T = 0.1, 0.55$ and different σ_{p^c} 's for hatch cover number (B)

VI. RESULT INTRUPTION

Analyzing the tables and figures in the previous section indicates that the effect of changing the standard deviation of the waterline on the failure probability and reliability is greater than the final strength. The values of reliability and failure probability indicate a greater reliability of the hatch cover of Panamax than the Handy size, despite its lower final strength.

Another significant result is the effect of the dispersion level or the standard deviation of the variables. The higher the standard deviation of the waterline and ultimate strength variables are, the greater the failure probability and the lower the reliability are. Consider the table 2. The value of reliability, for the same value of σ_T , is greater for $\sigma_{p^c} = 0.25$ than $\sigma_{p^c} = 2.5$. As an example, in this table, for $\sigma_T = 0.1$, $\sigma_{p^c} = 0.25$, the reliability value is equal to 0.9976 and for $\sigma_T = 0.1$, $\sigma_{p^c} = 2.5$, the reliability is equal to 0.92. That is, with increase in σ_{p^c} , the value of failure probability increases and reliability decreases, and this confirms the Interface Theory, as shown in Fig. 13.

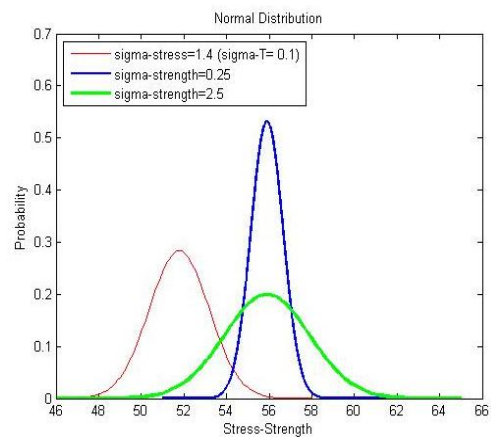


Fig. 13. curves of the reliability index, reliability, and failure probability for $\sigma_T = 0.1, 0.55$ and different σ_{p^c} 's for hatch cover number (B)

VII. CONCLUSION

The results of this research clearly show the effect of statistical values of parameters on the health index and reliability of the structure of the hatch cover. The effect of the dispersion of the standard deviation values on the reliability is very high,

Failure Probability and Reliability of Hatch Cover of Bulk Carrier Subjected To Lateral Pressure Load

which indicates that the accuracy in production and construction has a great impact on the failure probability and reliability. Considering the values of failure probability for the two types of hatch cover, indicates the impact of ship dimensional parameters such as waterline and height on the strength required for the hatch covers and shows that how much these values are effective in the design and the failure probability of hatch cover.

The concept of reliability can be used in designs and to modify the designs and previous rules.

For completion and continuation of this study, statistical analysis in the Ansys software can be used to calculate a more precise value of ultimate strength and include other statistical variables in the limit function and calculate more accurate values of failure probability and reliability. Reliability assessment can also be done by using SORM and Monte Carlo methods and compare the results with this method.

REFERENCES

1. Ship structures committee, <http://www.shipstructure.org/derby.shtml>, 15.9.2019
2. M. Zarei, . M. Zebardast, "ultimate strength analysis of hatch cover of bulk carrier", 11th national conference of marine industries of Iran, 2009.
3. International Convention of Load Lines, Annex I: Determinations for load lines, Regulation 15 in Chap. 11, 1966.
4. IACS: Evaluation of Scantlings of Hatch Covers of BulkCarrier Cargo Holds, IACS Requirement, 1997, vol. 1. 1997.
5. T. Yao, et. all, "Collapse strength of hatch cover of bulk carrier subjected to lateral pressure load", J. of Marine Structures, Vol. 16, 2003.
6. S-K. Choi, R. V. Grandhi and R. A. Canfield, 2007, Reliability-based Structural Design, Springer-Verlag London Limited 2007, PP. 80-151
7. A. M. Freudenthal, J. M. Garrelts, and M. Shinozuka, "The Analysis of Structural Safety," Journal of the Structural Division, ASCE, Vol. 92, No. ST1, 1966, pp. 267-325.
8. FSA of Bulk Carrier for end watertight integrity, Annex 4, Hatch cover failure scenarios, IACS, 2000.